

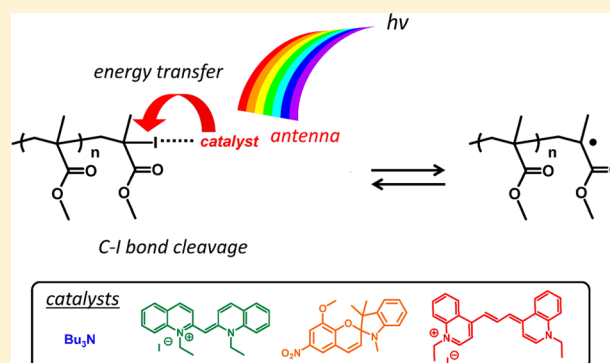
Photocontrolled Organocatalyzed Living Radical Polymerization Feasible over a Wide Range of Wavelengths

Akimichi Ohtsuki,[‡] Lin Lei,[‡] Miho Tanishima, Atsushi Goto,* and Hironori Kaji*

Institute for Chemical Research, Kyoto University, Uji, Kyoto 611-0011, Japan

S Supporting Information

ABSTRACT: Photocontrolled organocatalyzed living radical polymerization was conducted over a wide range of irradiation wavelengths (350–750 nm). The polymerization was induced and controlled at the desired wavelengths by exploiting suitable organic catalysts. This system was finely responsive to the irradiation wavelength; the polymerization was instantly switched on and off, and the polymerization rate was sensitively modulated by altering the irradiation wavelength. The polymer molecular weight and its distribution ($M_w/M_n = 1.1–1.4$) were well controlled for methacrylate monomers up to fairly high conversions in many cases. The monomer scope encompassed various functional methacrylates, and their block copolymers were obtained. The feasibility of such a wide range of wavelengths and the fine response to the wavelength are unprecedented features. As a unique application of the wavelength-responsive nature of this system, we demonstrated “one-pot” selective regulation of living radical polymerization and another type of polymerization (ring opening polymerization), where the regulation was achieved by simply altering the irradiation wavelength. Facile operation and applicability to a wide range of polymer designs are advantages of this polymerization.



INTRODUCTION

Photochemical reactions have been extensively exploited in organic chemistry and polymer chemistry.¹ The reactions do not require heat and are therefore applicable to functional groups and materials that decompose at high temperatures. A photochemical stimulus is one of the most useful external stimuli that can instantly switch the reactions “on” and “off” and can spatially trigger the reactions at specific positions and spaces. The reactions are also selectively inducible in response to the irradiation wavelengths; hence, multiple reactions may be regulated in one pot by simply altering the irradiation wavelength.

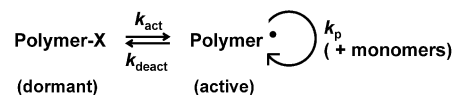
Our group is interested in the thermal and photochemical generation of a carbon-centered radical (R^\bullet) from an alkyl iodide ($R-I$) via organic catalysis. We applied this fundamental reaction to living radical polymerization (LRP) to synthesize well-defined polymers.^{2–6} We studied two reaction types. One was a reaction of $R-I$ with amine catalysts to generate R^\bullet .^{3–6} The catalyst initially coordinates with the iodine of $R-I$ to form a complex, and the $C-I$ bond of the complex is subsequently thermally or photochemically dissociated. Inspired by well-known relevant “irreversible” reactions,⁷ we explored the “reversible” reactions by exploiting appropriate catalysts, and we developed a novel LRP that we refer to reversible complexation-mediated polymerization (RCMP).^{3–6}

LRP has attracted increasing attention as an efficient tool for designing polymer architectures with predictable molecular weights and narrow molecular weight distributions.^{8–14}

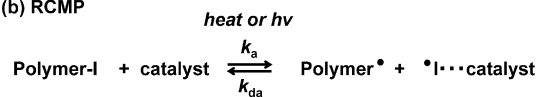
Mechanistically, LRP is based on the reversible activation of a dormant species (Polymer-X) to a propagating radical (Polymer $^\bullet$) (Scheme 1a). A sufficiently large number of

Scheme 1. Reversible Activation: (a) General Scheme and (b) RCMP

(a) Reversible activation (general scheme)



(b) RCMP



activation–deactivation cycles are required for achieving low polydispersity.¹⁵ In addition to thermal heating, photo irradiation has been utilized to control several LRP systems,¹⁶ e.g., with $X =$ nitroxides,¹⁷ (pseudo) halogens combined with metal^{18,19} and nonmetal²⁰ catalysts (atom transfer radical polymerization), dithioesters,^{21,22} tellurides,²³ iodine,²⁴ and cobalt complexes.²⁵ Photocontrolled LRP (photo LRP) is intriguing and opens up new applications. However, the

Received: March 12, 2015

Published: April 16, 2015

currently available systems are restricted in the wavelengths that can be used to control the polymerization. The feasible wavelength is nearly fixed in each system and is fundamentally determined by essential components (key elements and groups) contained in the capping agents and catalysts. Greater versatility with respect to wavelength could be highly beneficial for increasing the scope of photo LRP.

RCMP uses iodine as X (capping agent) and organic amines and organic salts as catalysts (Scheme 1b).^{3–6} Our LRP is unique in its first use of organic catalysts.^{2–6} An advantage of RCMP is that no special capping agents or metals are used. The catalysts are inexpensive, relatively nontoxic, easy to handle, and amenable to a variety of functional groups and monomers. RCMP is a facile and attractive methodology. Another useful feature is that RCMP can be controlled photochemically⁶ as well as thermally,^{3–5} as mentioned above. In our previous work, we utilized tributylamine (TBA) as a catalyst for photo-controlled RCMP (photo RCMP) (Scheme 2).⁶ We demon-

Scheme 2. Possible Mechanism of Photo RCMP



strated that this system is an ideal on–off switchable system by an external photo stimulus and that the polymerization speed is also finely tunable by the photo irradiation power.

RCMP is encouraging in that organic molecules with various structures can serve as catalysts.^{3–5} This aspect motivated us to utilize various organic molecules with different absorption wavelengths as catalysts in photo RCMP; thus, we undertook the aforementioned challenge concerning the restricted wavelengths. In this paper, we report photo RCMP feasible over a wide range of wavelengths, i.e., 350–750 nm. We selected suitable catalysts (Figure 1) to control the polymerization at

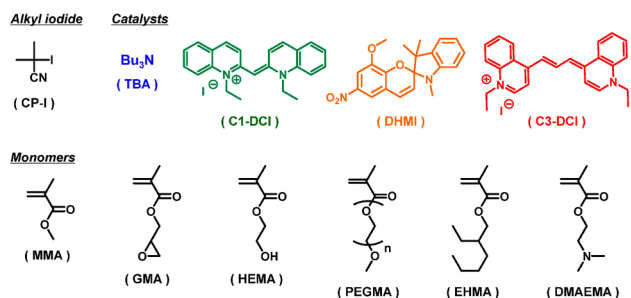
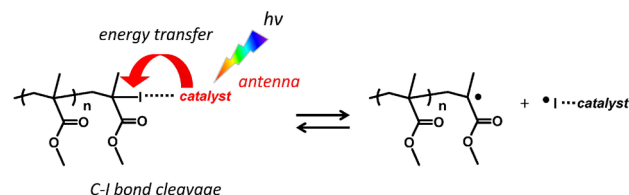


Figure 1. Structures of an alkyl iodide, catalysts, and monomers used in this work.

desired wavelengths. Prior to this study, wavelengths longer than 635 nm have never previously been utilized in any photo LRP systems. Feasibility over the whole visible region is unprecedented. We propose a mechanism in which the catalyst operates as an antenna that absorbs the light and transfers the energy to cleave the C–I bond of the complex (Scheme 3). (This mechanism is a tentatively postulated mechanism and the details need to be studied in the future.)

The studied catalysts (Figure 1) have advantages in their large extinction coefficients, commercial availability, and good compatibility with functional groups. These advantages offer a highly efficient, easily accessible, and versatile synthetic route. The monomer scope encompasses several functional methacrylates, and their block copolymers are obtainable. Taking

Scheme 3. C–I Bond Cleavage of Polymer Iodide via Light Absorption of Catalyst (Antenna) and Subsequent Energy Transfer



advantage of the wavelength-responsive nature of this system, we also pay attention to its unique application. We illustrate a “one-pot” synthesis of a block copolymer of methyl methacrylate (MMA) and δ -valerolactone (VL), in which LRP and ring-opening polymerization are selectively regulated in “one pot” by simply altering irradiation wavelength. Applicability to a wide range of polymer designs is a highly advantageous feature of this technique.

RESULTS AND DISCUSSION

Absorption Spectra. Figure 1 shows the structures and abbreviations of the initiating dormant species, i.e., 2-cyanopropyl iodide (CP-I), and the four catalysts, i.e., TBA, 1'-diethyl-2,2'-cyanine iodide (C1-DCI), 1',3'-dihydro-8-methoxy-1',3',3'-trimethyl-6-nitrospiro[2H-1-benzopyran-2,2'-(2H)-indole] (DHMI), and 1,1'-diethyl-4,4'-carbocyanine iodide (C3-DCI), studied in this work. Figure 2 shows the

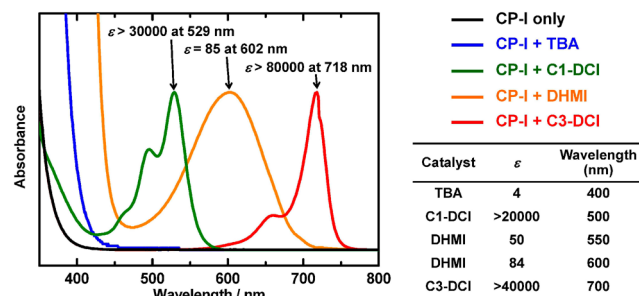


Figure 2. UV–vis–NIR spectra of CP-I (black line) and mixtures of CP-I and a catalyst in MMA at ambient temperature. The catalysts are TBA (blue line), C1-DCI (green line), DHMI (orange line), and C3-DCI (red line). The table and figure shows the extinction coefficients (ϵ) for mixtures of CP-I and a catalyst at the indicated wavelength.

absorption spectra of CP-I only and a mixture of CP-I and a catalyst. The solvent was bulk MMA in all cases. The spectrum of CP-I showed a peak at 280 nm that extended to approximately 400 nm (black line). A new shoulder peak appeared in the spectrum of the mixture of CP-I and TBA and ranged from 350 to 450 nm (blue line). This shoulder peak corresponds to a complex of CP-I and TBA.²⁶ Thus, we could use a wavelength between 350 and 450 nm for the TBA system. The mixtures of CP-I with C1-DCI (green line), DHMI (orange line), and C3-DCI (red line) exhibited longer absorption wavelengths. The peak maxima for these three mixtures were located at 530, 600, and 720 nm, respectively. With these catalysts, we could use longer wavelengths (>450 nm) to control the polymerization. The irradiation at 350–750 nm that was used in the following experiments gives an energy of 160–340 kJ mol^{−1}. This energy is sufficient to cleave the C–I bond whose dissociation energy is approximately 150 kJ

mol^{-1} .²⁷ The extinction coefficient (ϵ) was 4 at 400 nm with TBA, >20000 at 500 nm with C1-DCI, 50 at 550 nm with DHMI, 84 at 600 nm with DHMI, and >40000 at 700 nm with C3-DCI (Figure 2). The ϵ values for C1-DCI, DHMI, and C3-DCI are large.

We suppose that all of the four catalysts can complex with CP-I, as proved for TBA. However, the exact evidence for the complexation of C1-DCI, DHMI, and C3-DCI with CP-I was difficult to observe spectroscopically. The absorption spectra of the mixtures of these three catalysts with CP-I were very similar to those of the catalysts only (Supporting Information). In this regard, the complexation of these three catalysts with CP-I is not demonstrated yet, and the details need to be studied in the future.

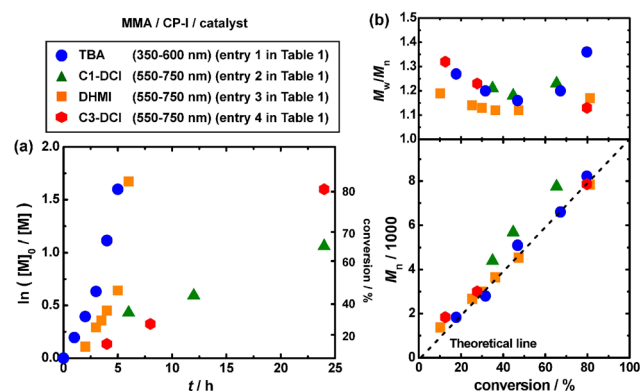


Figure 3. Plots of (a) $\ln([M]_0/[M])$ vs time t and (b) M_n and M_w/M_n vs conversion for the MMA/CP-I/catalyst systems (ambient temperature). For experimental conditions, see Table 1. The symbols are indicated in the figure.

Polymerizations of MMA. Figure 3 (circles) and Table 1 (entry 1) show the previously reported bulk polymerizations of MMA (100 equiv) containing CP-I (1 equiv) and TBA (0.25 equiv) irradiated at 350–600 nm at ambient temperature. In the present study, we attempted to use longer wavelengths. Figure 3 (triangles, squares, and pentagons) and Table 1 (entries 2–4) show the same polymerization but using C1-DCI (0.125 equiv), DHMI (0.5 equiv), or C3-DCI (0.25 equiv) as a catalyst with irradiation at 550–750 nm. The light source was a xenon lamp equipped with band-pass optical mirror and filter. The input electric power of the lamp and the exact light intensity at the reaction solution (as measured using a power meter) are given in Tables 1–3, 5, and 6. The polymerization was conducted in a test tube (with a diameter of 1 cm) under magnetic stirring. The test tube was immersed in silicone oil in a glass container to remove the heat of polymerization and the

heat of lamp from the test tube. The temperature of the oil was measured to be $25\text{ }^\circ\text{C} \pm 5\text{ }^\circ\text{C}$ in all studied polymerizations.

The polymerization proceeded to a high monomer conversion (65–81%) in all studied cases (Figure 3 and Table 1). Without a catalyst but with CP-I, no polymerization occurred, meaning that the polymerization required both CP-I and a catalyst. The first-order plot of the monomer concentration $[M]$ (Figure 3a) was linear until approximately 50% conversion, and at higher conversions, the polymerization rate R_p gradually increased because of a gel effect. The number-average molecular weight M_n agreed well with the theoretical value $M_{n,\text{theo}}$, and the polydispersity index ($\text{PDI} = M_w/M_n$, where M_w is the weight-average molecular weight) was as small as 1.2–1.3 from an early stage of polymerization. This result indicates that sufficiently fast dissociation of the C–I bond was induced by the photo irradiation. Importantly, PDI remained relatively small (approximately 1.2) up to high conversions. The control of M_n and PDI for the C1-DCI, DHMI, and C3-DCI systems at 550–750 nm was as good as that for the TBA system at 350–600 nm. These results clearly demonstrate the successful extension of the feasible wavelength to a longer-wavelength region.

In addition to broad bands, narrow bands of wavelengths, i.e., specific desired wavelengths, could also be applied. Because the absorption wavelength was complementary among the four catalysts, we were able to select suitable catalysts to desired wavelengths. Figure 4 and Table 2 (entries 1–5) show

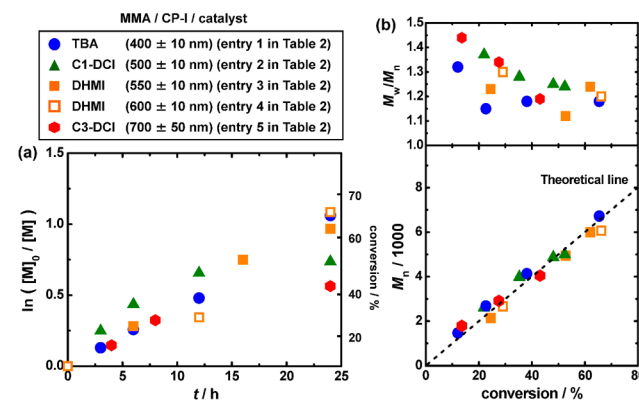


Figure 4. Plots of (a) $\ln([M]_0/[M])$ vs time t and (b) M_n and M_w/M_n vs conversion for the MMA/CP-I/catalyst systems (ambient temperature). For experimental conditions, see entries 1–5 in Table 2. The symbols are indicated in the figure.

controlled polymerizations at 400 (± 10) nm (TBA), 500 (± 10) nm (C1-DCI), 550 (± 10) nm (DHMI), 600 (± 10) nm (DHMI), and 700 (± 50) nm (C3-DCI). Compared with the R_p of the broad-band systems, the R_p in these cases was

Table 1. Polymerizations of MMA

entry	catalyst	wavelength (nm)	lamp electric power (W) ^a	light intensity at the solution (W/cm ²) ^b	$[MMA]_0/[CP-I]_0/[catalyst]_0$ (mM)	t (h)	conv (%)	M_n ($M_{n,\text{theo}}$)	PDI
1	TBA	350–600	60	0.19	8000/80/20	5	79	8200 (7900)	1.36
2	C1-DCI	550–750	150	0.23	8000/80/10 ^c	24	65	7800 (6500)	1.23
3	DHMI	550–750	150	0.23	8000/80/40	6	81	7800 (8100)	1.17
4	C3-DCI	550–750	150	0.23	8000/80/20 ^c	24	80	7900 (8000)	1.13

^aInput electricity power of xenon lamp. ^bActual light intensity (at the position of the reaction solution) experimentally measured by a power meter. The actual light intensity depends on the range of studied wavelength and the input electricity power. ^cDiluted with 25 wt % diglyme (MMA/diglyme = 75/25 wt %).

Table 2. Polymerizations of MMA at Narrow Bands of Wavelengths

entry	catalyst	wavelength (nm)	lamp electric power (W)	light intensity at the solution (W/cm ²)	[MMA] ₀ /[CP-I] ₀ /[catalyst] ₀ (mM)	t (h)	conv (%)	M _n (M _{n,theo})	PDI
1	TBA	400 ± 10	150	0.009	8000/80/40 ^a	24	65	6700 (6500)	1.18
2	C1-DCI	500 ± 10	300	0.017	8000/80/10 ^a	24	52	5000 (5200)	1.24
3	DHMI	550 ± 10	300	0.016	8000/80/40	24	62	6000 (6200)	1.24
4	DHMI	600 ± 10	300	0.022	8000/80/40	24	66	6000 (6600)	1.20
5	C3-DCI	700 ± 50	300	0.28	8000/80/20 ^a	24	43	4100 (4300)	1.19
6	C1-DCI	700 ± 50	300	0.28	8000/80/10 ^a	3	0	—	—
		600 ± 10	300	0.022		+3	10	1700 (1000)	1.34
		500 ± 10	300	0.017		+3	27	3000 (2700)	1.32
		400 ± 10	150	0.009		+3	35	3700 (3500)	1.29
7	C3-DCI	700 ± 50	300	0.28	8000/80/15 ^a	12	16	2000 (1600)	1.30
		600 ± 10	300	0.022		+3	16	2000 (1600)	1.30
		500 ± 10	300	0.017		+3	17	2100 (1700)	1.29
		400 ± 10	150	0.009		+3	21	2500 (2100)	1.25

^aDiluted with 25 wt % diglyme (MMA/diglyme = 75/25 wt %).

somewhat smaller because of the lower irradiation intensities (narrower bands); however, the R_p was still reasonably large. The monomer conversion reached 43–66% after 24 h while maintaining good control of the molecular weight in all cases. Thus, specific desired wavelengths were successfully applied.

Regarding the mechanism, Polymer-I could be activated not only by the supposed catalytic photolysis but also by degenerative chain transfer (DT) (activation with Polymer[•]).¹² However, DT is slow. The DT constant ($C_{ex} = 1.6$ for MMA)³ is so small that the DT mechanism only (iodide transfer polymerization) can not theoretically achieve a PDI < 1.7 in batch.¹⁵ To achieve low polydispersity, Polymer-I must be “frequently” activated by the photolysis, accompanied by a small contribution from DT.

Rate Control by Wavelength. Figure 5 and Table 2 (entries 6 and 7) demonstrate rate control by the irradiation

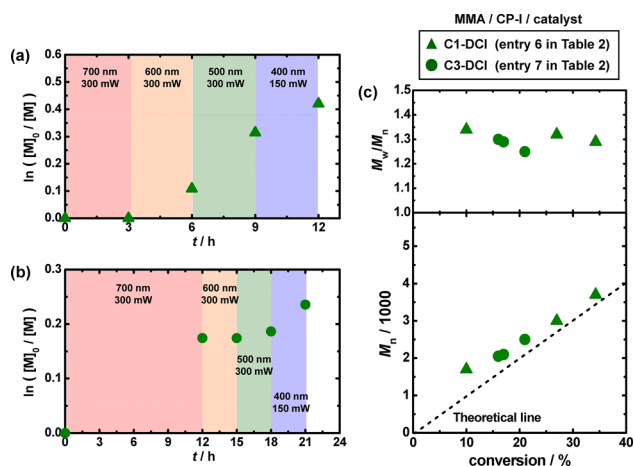


Figure 5. Plots of (a) and (b) $\ln([M]_0/[M])$ vs time t and (c) M_n and M_w/M_n vs conversion for the MMA/CP-I/catalyst systems (ambient temperature). For experimental conditions, see entries 6 and 7 in Table 2. The symbols are indicated in the figure.

wavelength. In the C1-DCI system, the irradiation wavelength was altered every 3 h from 700 nm to 600, 500, and 400 nm. Perfectly no polymerization occurred for the first 3 h because no light was absorbed at 700 nm. When the wavelength was altered to 600 nm, the system was switched “on”, and the polymerization smoothly proceeded. Importantly, R_p re-

sponded to the irradiation wavelength. At 600, 500, and 400 nm, the incremental conversion was 10, 17, and 8%, respectively, during each 3 h polymerization. Thus, the system was switched “on” and “off”, and R_p was finely tuned, according to the absorption intensity at each wavelength. A similar rate control was achieved using C3-DCI. The polymerization was switched “on” at 700 nm and “off” at 600 and 500 nm and resumed at 400 nm, in response to the wavelengths. The M_n and polydispersity were well controlled in both cases. These results demonstrate that efficient rate control was achieved by varying the irradiation wavelength.

Functional Monomers. An advantage of the catalysts used in the present study is their good compatibility with functional groups. Table 3 shows the polymerizations of several functional methacrylates with 2-ethylhexyl (EHMA), epoxide (GMA), hydroxyl (HEMA), poly(ethylene glycol) (PEGMA), and dimethylamino (DMAEMA) groups (Figure 1). We obtained hydrophobic and hydrophilic polymers with low polydispersity at the desired wavelengths of 400, 500, 550, and 700 nm. The R_p was larger for the functional monomers than for MMA in some cases, partly because the propagation rate constants k_p of the functional monomers²⁸ are larger than that of MMA.²⁹ This result demonstrates the good compatibility between the studied catalysts and various functional groups.

Chain-End Fidelity and Block Copolymerizations. To probe the livingness in this polymerization, we carried out elemental analysis and NMR analysis of the polymers obtained using DHMI at 550–750 nm, as shown in Figure 3 (squares). The polymers obtained at 3.5 and 6 h were purified by preparative gel permeation chromatography (GPC) to remove trace impurities such as residual catalyst. The M_n and PDI before and after the purification are listed in Table 4. The M_n and PDI were determined by GPC calibrated with PMMA standards.

Table 4 shows the elemental analysis results for the two polymers after purification. $I(\text{exp})$ is the experimentally determined iodine content, and $I(\text{theo})$ is the iodine content that was theoretically calculated from the M_n determined by GPC. The fraction of iodine chain end was calculated by $I(\text{exp})/I(\text{theo})$. This result shows that the polymers obtained at 3.5 h (30% conversion) and 6 h (81% conversion) included high fractions, i.e., 99% and 91%, respectively, of active polymer possessing iodine at the chain end (with $\pm 5\%$ experimental error).

Table 3. Polymerizations of Functional Monomers

entry	monomer	catalyst	wavelength (nm)	lamp electric power (W)	light intensity at the solution (W/cm ²)	$[\text{monomer}]_0/[\text{CP-I}]_0$ (mM)	t (h)	conv (%)	M_n^a ($M_{n,\text{theo}}$)	PDI ^a
1	HEMA	TBA	400 ± 10	60	0.004	8000/80/20	4	60	11000 (7800)	1.40
2	HEMA	DHMI	550 ± 10	300	0.016	8000/80/10 ^b	24	67	13000 (8700)	1.17
3	GMA	C1-DCI	500 ± 10	300	0.017	8000/80/20 ^c	24	72	8300 (11000)	1.11
4	GMA	C3-DCI	700 ± 50	300	0.28	8000/80/20 ^c	12	95	12000 (13000)	1.29
5	PEGMA ^d	C1-DCI	500 ± 10	300	0.017	8000/80/10	16	41	15000 (12000)	1.37
6	PEGMA ^d	DHMI	550 ± 10	300	0.016	8000/80/10	4	48	19000 (14000)	1.44
7	EHMA	TBA	400 ± 10	150	0.009	8000/80/40	12	69	11000 (14000)	1.11
8	EHMA	C1-DCI	500 ± 10	300	0.017	8000/80/10 ^c	6	53	9700 (11000)	1.39
9	EHMA	DHMI	550 ± 10	300	0.016	8000/80/40	6	71	10000 (14000)	1.07
10	EHMA	C3-DCI	700 ± 50	300	0.28	8000/80/20 ^c	24	75	14000 (15000)	1.12
11	DMAEMA	TBA	400 ± 10	60	0.004	8000/80/20	3.5	71	9000 (11000)	1.45
12	DMAEMA	C1-DCI	500 ± 10	300	0.017	8000/80/10 ^b	24	71	11000 (11000)	1.40
13	DMAEMA	C3-DCI	700 ± 50	300	0.28	8000/80/20	6	53	7900 (8500)	1.30

^aDetermined by GPC with a MALLS detector. ^bAddition of I₂ (1 mM). ^cDiluted with 25 wt % diglyme (monomer/diglyme = 75/25 wt %).

^dMolecular weight of monomer = 300.

Table 4. Elemental Analysis of Polymers Obtained in Figure 4 (Squares)

time (h)	purification	M_n	PDI	$I(\text{exp})$ (%)	$I(\text{theo})$ (%)	fraction of iodide chain end (%)
3.5	before	3000	1.13			
	after	3100	1.13	4.03	4.09	99
6	before	7800	1.17			
	after	8000	1.16	1.44	1.58	91

The polymer obtained at 3.5 h was analyzed, after purification, by high-resolution 800 MHz ¹H NMR spectroscopy (Figure 6). The methyl protons (a, a', and a'') at the side

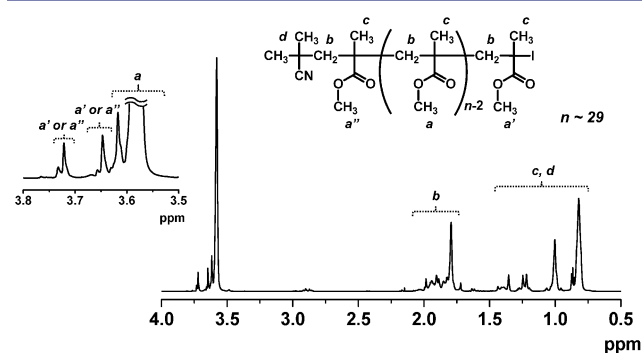


Figure 6. ¹H NMR spectrum (in the range of 0.5–4.0 ppm) of the polymer for 3.5 h after purification in Table 4 (in CDCl₃).

chain appeared at 3.55–3.75 ppm. The main peak at 3.55–3.60 ppm and its side peak at 3.60–3.63 ppm were assigned to the monomer units (a) in the middle of the chain. The side peak at

3.60–3.63 ppm may be due to a chain-end penultimate unit. The downfield-shifted peak at 3.71–3.75 ppm would be assigned to the ω-terminal chain-end unit (a') adjacent to iodine.^{4,30} On the basis of the peak area and the M_n determined by GPC, the fraction of iodine chain end was calculated to be ~100% (calculated to be 102% with ±10% experimental error). The peak at 3.63–3.67 ppm would be attributable to the α-terminal chain-end unit (a'') adjacent to the 2-cyanopropyl (CP) group. However, this assignment is not definitive, and the peak at 3.63–3.67 ppm could also be assigned to the ω-terminal chain-end unit (a'). In this case, the fraction of iodine chain end was calculated to be 102%. The elemental analysis and NMR analysis demonstrate good livingness (high chain-end fidelity) in this polymerization.

Taking advantage of this good livingness, we prepared block copolymers. We synthesized a macroinitiator, poly(methyl methacrylate)-iodide (PMMA-I), using DHMI under the condition shown in Figure 3 (squares); the reaction was run for 3.5 h. The obtained purified macroinitiator ($M_n = 3100$ and PDI = 1.13) was used in the polymerizations of HEMA, GMA, PEGMA, and DMAEMA, to successfully afford the desired block copolymers (Table 5). The GPC chromatograms showed that little starting macroinitiator was present in the products (Figure 7), indicating efficient block copolymer formation.

Selective Control of Two Polymerizations by Wavelength. Selective control of multiple reactions by the irradiation wavelength is a unique application of photo reactions. An example described here of photo RCMP is a "one-pot" synthesis of a block copolymer of MMA and VL (Scheme 4). RCMP and ring-opening polymerization (ROP) were selectively regulated in one pot by simply altering the irradiation wavelength. We utilized a dual initiator, 2-

Table 5. Block Copolymerizations of Functional Methacrylates from PMMA-I Macroinitiator ($M_n = 3100$, PDI = 1.13)

entry	monomer	catalyst	wavelength (nm)	lamp electric power (W)	light intensity at the solution (W/cm ²)	$[\text{monomer}]_0/[\text{PMMA-I}]_0$ (mM)	t (h)	conv (%)	M_n^a ($M_{n,\text{theo}}$)	PDI ^a
1	HEMA	DHMI	550 ± 10	280	0.016	8000/80/10 ^b	10	98	15000 (16000)	1.34
2	GMA	C1-DCI	500 ± 10	300	0.017	8000/80/20 ^c	20	69	12000 (13000)	1.26
3	PEGMA ^d	DHMI	550 ± 10	300	0.017	8000/80/10	2	64	11000 (22000)	1.22
4	DMAEMA	C3-DCI	700 ± 50	300	0.28	8000/80/20	5	67	16000 (14000)	1.40

^aDetermined by GPC with a PMMA calibration (eluent = THF in all cases). ^bDiluted with 40 wt % ethanol. ^cDiluted with 25 wt % diglyme (MMA/diglyme = 75/25 wt %). ^dMolecular weight of monomer = 300.

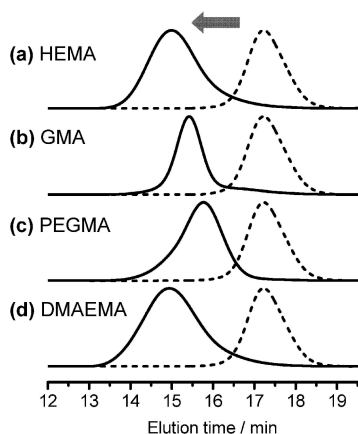
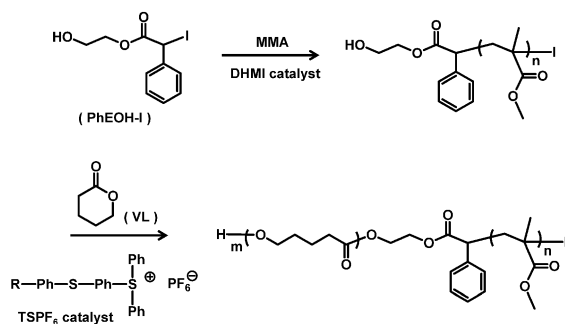


Figure 7. GPC chromatograms before (dashed lines) and after (solid lines) the block copolymerization in Table 5. Entries 1–4 in Table 5 corresponds to (a–d) in the figure, respectively.

Scheme 4. Synthesis of a Block Copolymer of MMA and VL



hydroxyethyl 2-iodo-2-phenylacetate (PhEOH-I) (Scheme 4), which possesses both iodine to initiate RCMP and a hydroxyl group to initiate ROP. The mixture of MMA (25 equiv), VL (25 equiv), PhEOH-I (1 equiv), DHMI (0.06 equiv), an ROP catalyst (a photo acid generator, triarylsulfonium hexafluorophosphate (TSPF₆) (Scheme 4))³¹ (0.002 equiv), and a solvent (propylene carbonate) was subjected to polymerization. The absorption spectrum of the mixture (Figure 8a) suggested that 550–750 nm (absorbed by DHMI) and 350–380 nm (absorbed by TSPF₆) were feasible for selectively inducing RCMP and ROP, respectively.

The mixture was first irradiated at 550–750 nm for 6 h for obtaining the first block segment (Table 6 and Figures 8b,c and 9). The monomer conversions of MMA and VL were 67% and 0%, respectively, showing that RCMP of MMA selectively occurred at this wavelength. The M_n (= 2200) agreed well with $M_{n,theor}$, and PDI was as small as 1.09. The irradiation wavelength was subsequently altered to 350–380 nm for obtaining the second block segment. After 2 h, the incremental monomer conversions of MMA and VL were 1% and 80%, respectively, demonstrating that ROP of VL selectively occurred at this wavelength. The GPC chromatograms clearly show that the polymer chain smoothly extended (Figure 8c) and that a well-defined block copolymer (M_n = 4200 and PDI = 1.20) was obtained.

The ¹H NMR spectra further confirm this selectivity (Figure 9). We observed only PMMA after the first block copolymerization at 6 h (Figure 9b), and perfectly no poly(δ -valerolactone) was detected. The signal of the methine proton (c) at the RCMP initiating site (5.6 ppm) completely

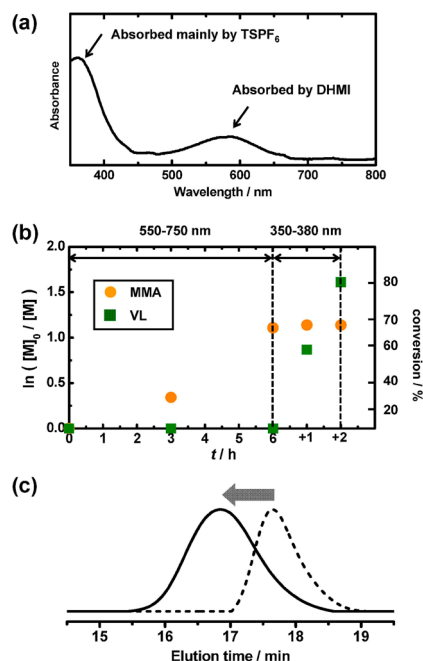


Figure 8. (a) UV–vis–NIR spectra of the mixture of DHMI and TSPF₆ in propylene carbonate. (b) Plot of $\ln([M]_0/[M])$ vs time t and (c) GPC chromatograms at 6 h and at additional 2 h for the polymerization in Table 6.

disappeared (Figure 9a,b), meaning quantitative initiation at the RCMP initiating site. The signal of the methylene protons (a) at the ROP initiating site (4.3 ppm) was broadened (because this site became the polymer chain-end) but remained (Figure 9a,b), suggesting an intact ROP initiating site. After the second block copolymerization at 1 h (Figure 9c), poly(δ -valerolactone) was clearly observed. The signal (a') (4.15–4.35 ppm) at the ROP initiating site was shifted to a higher magnetic field (a'') (4.1–4.2 ppm), meaning successful initiation at the ROP initiating site. No signal remaining at 4.2–4.35 ppm suggests a high block efficiency. The degree of polymerization on the basis of the peak area (PhEOH-I initiator (signal (d)) vs polymer) agreed well with the M_n determined by GPC (within 15%) for these polymers (Figure 9b,c). In this way, we selectively regulated two reactions in one pot by simply altering the irradiation wavelength.

CONCLUSIONS

Photo RCMP was successfully applied in a wide range of irradiation wavelengths (350–750 nm). The polymerization was induced and controlled at desired wavelengths by exploiting suitable catalysts. This system was finely responsive to the irradiation wavelength; the polymerization was instantly switched on and off, and R_p was sensitively modulated by the irradiation wavelength. This polymerization was compatible with various functional monomers, and their block copolymers were obtained. A block copolymer of MMA and VL was obtained in one pot by selectively regulating LRP and ring-opening polymerization by altering the irradiation wavelength. An advantage of this system is that no special capping agents or metals are used; in addition, the catalysts are commercially available. The facile operation, fine response to wavelength, and applicability to a large variety of polymer designs may be greatly beneficial in a variety of applications. An important future application could be surface-initiated photo RCMP. Patterned

Table 6. Block Copolymerizations of MMA and VL ($[MMA]_0/[VL]_0/[PhEOH-I]_0/[TSPF_6]_0/[DHMI]_0 = 4000/4000/160/0.25/10 \text{ mM}$)^a

entry	wavelength (nm)	lamp electric power (W)	light intensity at the solution (W/cm ²)	t (h)	conv (MMA) ^b (%)	conv (VL) ^b (%)	M _n ^c (M _{n,theo})	PDI ^c
1	550–750	150 ^d	0.23	3	29	0	1500 (600)	1.08
				6	67	0	2200 (2000)	1.09
	350–380	LED lamp ^d	0.38	+1	68	58	3600 (3500)	1.19
				+2	68	80	4200 (4000)	1.20

^aDiluted with 20 wt % propylene carbonate (monomers/propylene carbonate = 80/20 wt %). ^bDetermined by high performance liquid chromatography. ^cDetermined by GPC with a PMMA calibration (eluent = THF in all cases). ^dxenon lamp at 550–750 nm and LED lamp at 350–380 nm.

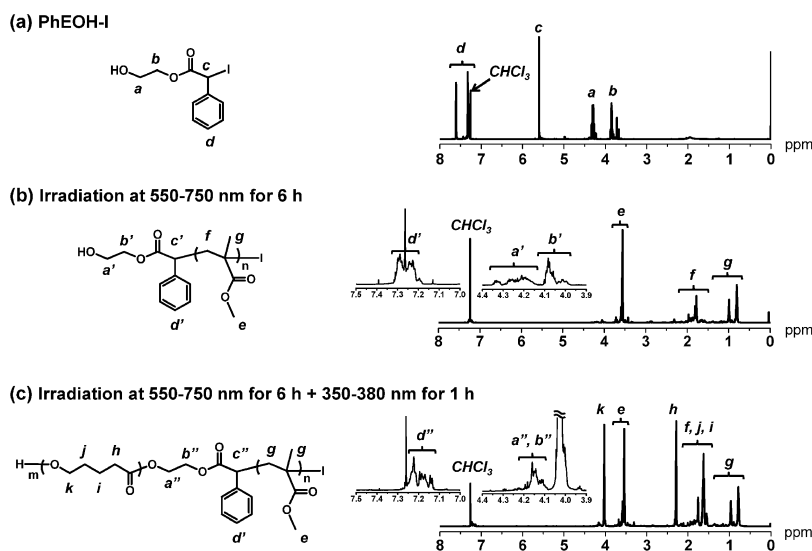


Figure 9. ¹H NMR spectra (CDCl₃ solvent) of (a) PhEOH-I, and polymers obtained (b) at 550–750 nm for 6 h and (c) at 550–750 nm for 6 h + 350–380 nm for 1 h in Table 6 (after purification for both polymers).

(possibly three-dimensional) polymer brushes can be created by photo lithography and interference lithography, taking advantage of the wavelength-responsive nature of our developed system. Such an application will be studied in our laboratory.

■ ASSOCIATED CONTENT

Supporting Information

Experimental section and UV–vis–NIR spectra of catalysts only. This material is available free of charge via the Internet at <http://pubs.acs.org>.

■ AUTHOR INFORMATION

Corresponding Authors

*agoto@scl.kyoto-u.ac.jp

*kaji@scl.kyoto-u.ac.jp

Author Contributions

‡These authors contributed equally.

Notes

The authors declare no competing financial interest.

■ ACKNOWLEDGMENTS

This work was supported by Grants-in-Aid for Scientific Research from the Japan Society of the Promotion of Science (JSPS), and the Japan Science and Technology Agency (JST). PhEOH-I was provided through the courtesy of Godo Shigen Co., LTD, Japan. High-resolution 800 MHz NMR spectra (Figures 6 and 9) were acquired with the NMR spectrometer in

the Joint Usage/Research Center (JURC) at Institute for Chemical Research, Kyoto University.

■ REFERENCES

- (1) (a) Adzima, B. J.; Tao, Y.; Kloxin, C. J.; DeForest, C. A.; Anseth, K. S.; Bowman, C. N. *Nat. Chem.* **2011**, *3*, 256–259. (b) Brieke, C.; Rohrbach, F.; Gottschalk, A.; Mayer, G.; Heckel, A. *Angew. Chem., Int. Ed.* **2012**, *51*, 8446–8476. (c) Wylie, R. G.; Ahsan, S.; Aizawa, Y.; Maxwell, K. L.; Morshead, C. M.; Shoichet, M. S. *Nat. Mater.* **2011**, *10*, 799–806. (d) Liu, Z.; Liu, T.; Lin, Q.; Bao, C.; Zhu, L. *Angew. Chem., Int. Ed.* **2015**, *54*, 174–178.
- (2) (a) Goto, A.; Zushi, H.; Hirai, N.; Wakada, T.; Tsujii, Y.; Fukuda, T. *J. Am. Chem. Soc.* **2007**, *129*, 13347–13354. (b) Goto, A.; Hirai, N.; Wakada, T.; Nagasawa, K.; Tsujii, Y.; Fukuda, T. *Macromolecules* **2008**, *41*, 6261–6264. (c) Goto, A.; Hirai, N.; Nagasawa, K.; Tsujii, Y.; Fukuda, T.; Kaji, H. *Macromolecules* **2010**, *43*, 7971–7978. (d) Vana, P.; Goto, A. *Macromol. Theory Simul.* **2010**, *19*, 24–35. (e) Yorizane, M.; Nagasuga, T.; Kitayama, Y.; Tanaka, A.; Minami, H.; Goto, A.; Fukuda, T.; Okubo, M. *Macromolecules* **2010**, *43*, 8703–8705.
- (3) Goto, A.; Suzuki, T.; Ohfuji, H.; Tanishima, M.; Fukuda, T.; Tsujii, Y.; Kaji, H. *Macromolecules* **2011**, *44*, 8709–8715.
- (4) Goto, A.; Ohtsuki, A.; Ohfuji, H.; Tanishima, M.; Kaji, H. *J. Am. Chem. Soc.* **2013**, *135*, 11131–11139.
- (5) (a) Lei, L.; Tanishima, M.; Goto, A.; Kaji, H. *Polymers* **2014**, *6*, 860–872. (b) Lei, L.; Tanishima, M.; Goto, A.; Kaji, H.; Yamaguchi, Y.; Komatsu, H.; Jitsukawa, T.; Miyamoto, M. *Macromolecules* **2014**, *47*, 6610–6618.
- (6) Ohtsuki, A.; Goto, A.; Kaji, H. *Macromolecules* **2013**, *46*, 96–102.
- (7) (a) Stevenson, D. P.; Coppinger, G. M. *J. Am. Chem. Soc.* **1962**, *84*, 149–152. (b) Lautenberger, W. J.; Jones, E. N.; Miller, J. G. *J. Am. Chem. Soc.* **1968**, *90*, 1110–1115. (c) Ishibashi, H.; Haruki, S.;

Uchiyama, M.; Tamura, O.; Matsuo, J. *Tetrahedron Lett.* **2006**, *47*, 6263–6266.

(8) (a) Matyjaszewski, K.; Möller, M. *Polymer Science: A Comprehensive Reference*; Elsevier: Amsterdam, 2012. (b) Tsarevsky, N. V.; Sumerlin, B. S. *Fundamentals of Controlled/Living Radical Polymerization*; Royal Society of Chemistry: U.K., 2013.

(9) Nicolas, J.; Guillauneuf, Y.; Lefay, C.; Bertin, D.; Gigmes, D.; Charleux, B. *Prog. Polym. Sci.* **2013**, *38*, 63–235.

(10) (a) Matyjaszewski, K.; Tsarevsky, N. V. *J. Am. Chem. Soc.* **2014**, *136*, 6513–6533. (b) Ouchi, M.; Terashima, T.; Sawamoto, M. *Chem. Rev.* **2009**, *109*, 4963–5050. (c) Zhang, N.; Samanta, S. R.; Rosen, B. M.; Percec, V. *Chem. Rev.* **2014**, *114*, 5848–5958.

(11) Keddie, D. J.; Moad, G.; Rizzardo, E.; Thang, S. H. *Macromolecules* **2012**, *45*, 5321–5342.

(12) David, G.; Boyer, C.; Tonnar, J.; Ameduri, B.; Lacroix-Desmazes, P.; Boutevin, B. *Chem. Rev.* **2006**, *106*, 3936–3962.

(13) Yamago, S. *Chem. Rev.* **2009**, *109*, 5051–5068.

(14) (a) Zetterlund, P. B.; Kagawa, Y.; Okubo, M. *Chem. Rev.* **2008**, *108*, 3747–3794. (b) Satoh, K.; Kamigaito, M. *Chem. Rev.* **2009**, *109*, 5120–5156. (c) Monteiro, M. J.; Cunningham, M. F. *Macromolecules* **2012**, *45*, 4939–4957.

(15) For reviews on kinetic of LRP: (a) Fukuda, T. *J. Polym. Sci., Part A: Polym. Chem.* **2004**, *42*, 4743–4755. (b) Fischer, H. *Chem. Rev.* **2001**, *101*, 3581–3618. (c) Goto, A.; Fukuda, T. *Prog. Polym. Sci.* **2004**, *29*, 329–385.

(16) For a review on photo LRP: Yamago, S.; Nakamura, Y. *Polymer* **2013**, *54*, 981–994.

(17) (a) Scaiano, J. C.; Connolly, T. J.; Mohtat, N.; Pliva, C. N. *Can. J. Chem.* **1997**, *75*, 92–97. (b) Goto, A.; Scaiano, J. C.; Maretta, L. *Photochem. Photobiol. Sci.* **2007**, *6*, 833–835. (c) Guillauneuf, Y.; Bertin, D.; Gigmes, D.; Versace, D.-L.; Lalevée, J.; Fouasseir, J.-P. *Macromolecules* **2010**, *43*, 2204–2212. (d) Versace, D.-L.; Guillauneuf, Y.; Bertin, D.; Fouasseir, J.-P.; Lalevée, J.; Gigmes, D. *Org. Biomol. Chem.* **2011**, *9*, 2892–2898.

(18) (a) Kwak, Y.; Matyjaszewski, K. *Macromolecules* **2010**, *43*, 5180–5183. (b) Tasdelen, M. A.; Uygen, M.; Yagci, Y. *Macromol. Rapid Commun.* **2011**, *32*, 58–62. (c) Mosnáček, J.; Ilčíková, M. *Macromolecules* **2011**, *45*, 5859–5865. (d) Konkolewicz, D.; Schröder, K.; Buback, J.; Bernhard, S.; Matyjaszewski, K. *ACS Macro Lett.* **2012**, *1*, 1219–1223.

(19) (a) Fors, B. P.; Hawker, C. J. *Angew. Chem., Int. Ed.* **2012**, *51*, 8850–8853. (b) Poelma, J. E.; Fors, B. P.; Meyers, G. F.; Kramer, J. W.; Hawker, C. J. *Angew. Chem., Int. Ed.* **2013**, *52*, 6844–6848. (c) Xu, J.; Jung, K.; Atme, A.; Shanmugam, S.; Boyer, C. *J. Am. Chem. Soc.* **2014**, *136*, 5508–5519.

(20) (a) Treat, N. J.; Sprafke, H.; Kramer, J. W.; Clark, P. G.; Barton, B. E.; de Alaniz, J. R.; Fors, B. P.; Hawker, C. J. *J. Am. Chem. Soc.* **2014**, *136*, 16096–16101. (b) Miyake, G. M.; Theriot, J. C. *Macromolecules* **2014**, *47*, 8255–8261.

(21) Otsu, T.; Yoshida, M.; Tazaki, T. *Makromol. Chem., Rapid Commun.* **1982**, *3*, 127–132.

(22) (a) Quinn, J. F.; Barner, L.; Barner-Kowollik, C.; Rizzardo, E.; Davis, T. P. *Macromolecules* **2002**, *35*, 7620–7627. (b) You, Y.; Hong, C.; Bai, R.; Pan, C.; Wang, J. *Macromol. Chem. Phys.* **2002**, *203*, 477–483. (c) Muthukrishnan, S.; Pan, E. H.; Stenzel, M. H.; Barner-Kowollik, C.; Davis, T. P.; Lewis, D.; Barner, L. *Macromolecules* **2007**, *40*, 2978–2980. (d) Su, X.; Zhao, Z.; Li, H.; Li, X.; Wu, P.; Han, Z. *Eur. Polym. J.* **2008**, *44*, 1849–1856. (e) Tasdelen, M. A.; Durmaz, Y. Y.; Karagoz, B.; Bicak, N.; Yagci, Y. *J. Polym. Sci., Part A: Polym. Chem.* **2008**, *46*, 3387–3395. (f) Zhou, H.; Johnson, J. A. *Angew. Chem., Int. Ed.* **2013**, *52*, 2235–2238. (g) Shanmugam, S.; Xu, J.; Boyer, C. *Chem. Sci.* **2015**, *6*, 1341–1349.

(23) (a) Yamago, S.; Ukai, Y.; Matsumoto, A.; Nakamura, Y. *J. Am. Chem. Soc.* **2009**, *131*, 2100–2101. (b) Nomura, A.; Goto, A.; Ohno, K.; Kayahara, E.; Yamago, S.; Tsujii, Y. *J. Polym. Sci., Part A: Polym. Chem.* **2011**, *49*, 5284–5292. (c) Nakamura, Y.; Arima, T.; Tomita, S.; Yamago, S. *J. Am. Chem. Soc.* **2012**, *134*, 5536–5539.

(24) Wolpers, A.; Vana, P. *Macromolecules* **2014**, *47*, 954–953.

(25) (a) Detrembleur, C.; Versace, D.; Piette, Y.; Hurtgen, M.; Jérôme, C.; Lalevée, J.; Debuigne, A. *Polym. Chem.* **2012**, *3*, 1856–1866. (b) Zhao, Y.; Yu, M.; Fu, X. *Chem. Commun.* **2013**, *49*, 5186–5188.

(26) (a) Stevenson, D. P.; Coppinger, G. M. *J. Am. Chem. Soc.* **1962**, *84*, 149–152. (b) Lautenberger, W. J.; Jones, E. N.; Miller, J. G. *J. Am. Chem. Soc.* **1968**, *90*, 1110–1115. (c) Cossy, J.; Ranaivossata, J.; Bellosta, V. *Tetrahedron Lett.* **1994**, *44*, 8161–8162.

(27) Lin, C. Y.; Coote, M. L.; Gennaro, A.; Matyjaszewski, K. *J. Am. Chem. Soc.* **2008**, *130*, 12762–12774.

(28) (a) Beuermann, S.; Buback, M.; Davis, T. P.; García, N.; Gilbert, R. G.; Hutchinson, R. A.; Kajiwar, A.; Kamachi, M.; Lacić, I.; Russell, G. T. *Macromol. Chem. Phys.* **2003**, *204*, 1338–1350. (b) Beuermann, S.; Buback, M.; Davis, T. P.; Gilbert, R. G.; Hutchinson, R. A.; Kajiwar, A.; Klumperman, B.; Russell, G. T. *Macromol. Chem. Phys.* **2000**, *201*, 1355–1364. (c) Buback, M.; Kurz, C. H. *Macromol. Chem. Phys.* **1998**, *199*, 2301–2310.

(29) Beuermann, S.; Buback, M.; Davis, T. P.; Gilbert, R. G.; Hutchinson, R. A.; Olaj, O. F.; Russell, G. T.; Schweer, J.; van Herk, A. M. *Macromol. Chem. Phys.* **1997**, *198*, 1545–1560.

(30) Ando, T.; Kamigaito, M.; Sawamoto, M. *Macromolecules* **1997**, *30*, 4507–4510.

(31) Barker, I. A.; Dove, A. P. *Chem. Commun.* **2013**, *49*, 1205–1207.